Influence of the gelator structure and solvent on the organisation and chirality of self-assembling fibrillar networks†

Quoc Nghi Pham,[a] Nicolas Brosse,[b] Céline Frochot,[c] Dominique Dumas,[d] Alexandre Hocquet[a] and Brigitte Jamart-Grégoire*[a]

Received (in Montpellier, France) 18th September 2007, Accepted 8th January 2008
First published as an Advance Article on the web 5th February 2008
DOI: 10.1039/b714375c

Chromophoric probes of naphthalimide moieties enable evaluation of their assembling behaviour photophysically through fluorescence spectroscopy and microscopy, and circular dichroism. These experiments highlight the influence of the nature of the chemical substitution of the organogelator. Very interesting results were also obtained by performing CD experiments showing that the nature of the solvent should modify the chirality of self-assembled aggregates. Highly oriented network structures were observed in the gel state and disappeared in isotropic solution. Microfibrous self-aggregation of organogels is *in situ* observed *via* fluorescence and SHG imaging and confirmed by transmission electron microscopic analysis of the dried sample.

Introduction

Low-molecular-mass molecules exhibiting organogelation are receiving increasing attention[1] because of their current and future applications in areas such as entrapment of biomolecules,[2a] separation,[2b] photo-responsive material,[2c] biomimetics.[2d] Moreover, gelling agents (gelators) bearing π-conjugated molecular structure have attracted much interest because of their potential applications in optoelectronic fields (fluorescence, sensing ability *etc.*).

Organogels are generally formed by a self-aggregation of gelators, leading to the formation of fibrous three-dimensional networks with cross-links among the nanofibers entrapping the solvent.[3] Terech and Weiss have extensively studied these soft materials and explored their physicochemical properties essentially by rheology, light scattering and microscopy.[1a]

In the fibers, gelator molecules are self-assembled through non-covalent interactions[1a,4] (hydrogen bonding, van der Waals, π-stacking...) with a strong self-complementarity and unidirectional intermolecular cohesion. Indeed, gelator–solvent interactions[5] sometimes seem to influence the molecular arrangement, the morphology of the fibers and the junction zones.

Several examples of amino acid-type organogelators, such as small peptides or pseudopeptides,[6] cyclopeptides[7] and urea or bis-urea,[8] have been previously reported in the literature and have been studied as models for hydrogen-bonding type organogelators. However, the relationship between the chemical structure of an organogelator and its gelation properties in a given solvent is not clearly established; not only does the discovery of new gelators remain mainly fortuitous but a very small structural or chemical variation of the molecule can result in a drastic change of its gelation properties. In this context, a better understanding of this phenomenon is of great interest.

In a preliminary communication, we described a new family of (*S*)-amino acid type gelators obtained *via* an easy and inexpensive route.[9] These novel gelators are very easily prepared from cheap starting materials and allowed many structural variations of the side chain R. In order to go deeply into the organogelation phenomenon, in this paper we turn our attention to the self-assembling behaviour of two gelators (compounds **1** and **2**, see Chart 1) which bear a fluorescent chromophore (a naphthalimide moiety) using circular dichroism (CD), fluorescence spectroscopy and microscopy and molecular simulation. We study simultaneously the effect of the gelator structure and the nature of the solvent on the molecular arrangement and the aggregate structures. The macroscopic structure of the aggregates is indeed observed by using fluorescence and second harmonic generation (SHG) imaging and transmission electron microscopy.

Results and discussion

1 Gelation studies

Compounds **1** and **2** were first studied with regard to their gelation behaviour in various apolar solvents.

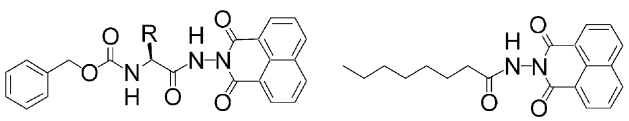

1 R= CH_2-$CH(CH_3)_2$
2 R= CH_2-C_6H_5

Ref **A**

Chart 1 Formula of organogelator molecules **1** and **2** and reference compound **A**.

[a] *Laboratoire de Chimie Physique Macromoléculaire (LCPM), Nancy-Université, CNRS, UMR 7568, 1 rue Grandville BP 451, 54001 Nancy, France*
[b] *Laboratoire d'Etude et de Recherche sur le Matériau Bois, Nancy-Université, Bd. des Aiguillettes, BP 239, 54506 Vandoeuvre-les-Nancy, France*
[c] *Département de Chimie Physique des Réactions, Nancy-Université, CNRS, UMR 7630, 1 rue Grandville BP 451, 54001 Nancy, France*
[d] *Laboratoire d'Energétique et de Mécanique Théorique et Appliquée, Nancy-Université, CNRS, UMR 7563, 9 av. de la Forêt de Haye, 54505 Vandoeuvre-les-Nancy, France*

† Electronic supplementary information (ESI) available: UV-vis spectra of **2** in toluene. See DOI: 10.1039/b714375c

Thermoreversible gels were obtained with many different organic solvents at low concentration; depending on the structural variation of the side chain R, the gels obtained were either clear (CG) or turbid (TG) and their properties were first evaluated with regard to two factors:

(1) the critical gelation concentration (CGC in wt%) for which the solution changes into a gel phase (stable at room temperature),

(2) the gel–solution phase transition temperature (T_{gs} in °C) at which the gel melts into solution, established by the "falling-ball" method.

The "temperature *versus* concentration" phase diagrams for the gelators **1** and **2** in toluene are shown in Fig. 1. We observe a nearly linear variation of the T_{gs} values as a function of the concentration. Regardless of the gelator concentration, the T_{gs} for gelator **1** is always lower than that for gelator **2**. Previous results of our group[9] showed that the CGC of **1** in toluene is 0.5 wt% whereas that of **2** in toluene is much lower, around 0.18 wt%. These differences come from the chemical difference in the organogelators (the substituted side chain R is an alkyl for **1** and a phenyl for **2**) and not from the small difference in their molecular weight. We suppose that the presence of an aromatic group reinforces probably the intermolecular interactions *via* π-stacking.

The "falling ball" method, while very convenient to perform, probably suffers from sensitivity to the measuring parameters (size and weight of the ball, diameter of the tube). In the vicinity of the melting temperature, the mesh is very loose, fragile and can be fractured by the gravity effect applied to the ball. Experimentally, simple precautions have to be taken such as the use of a tube with a diameter large enough, with respect to that of the ball, to prevent undesirable wall effects. Practically, the need for a clear response (*i.e.*, ball "felt" or "still in position") requires a surrounding temperature approach broad enough, as well as a ball heavy enough, to avoid intermediate situations of the ball which would be difficult to interpret. One can reasonably say that the results obtained represent "macroscopic" disaggregating points, and these melting temperatures are often lower than those obtained from spectroscopic techniques. Therefore, we used other techniques to determine the T_{gs} values. The results are gathered in Table 1. As expected, these T_{gs} values are higher than those obtained from the "falling ball" method, for the same concentration.

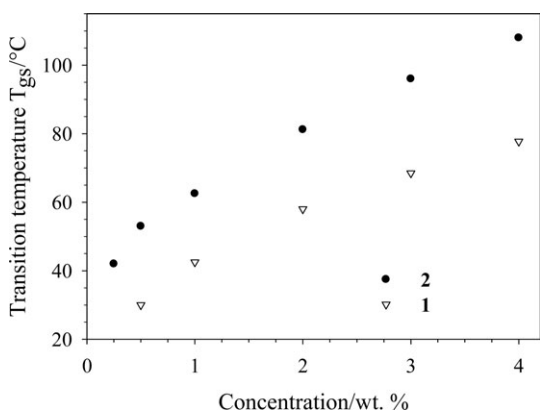

Fig. 1 Phase diagrams of gelators **1** and **2** in toluene.

Table 1 Melting temperatures, determined by different techniques for gelators **1** and **2** in toluene

Technique	Gelator **1**		Gelator **2**	
	c (wt%)	T_{gs}/°C	c (wt%)	T_{gs}/°C
DSC			4.00	104
Classical rheology[9]	0.50	45	0.50	80
Fluorescence spectroscopy	0.50	~30	0.21	43
	0.93	48	0.25	46
Circular dichroism	0.50	<40	0.20	~45

2 Fluorescence spectroscopy and microscopy

Fluorescence spectroscopy is a powerful tool which can be used as an optical method well suited to give information on the organization of macromolecules in aqueous or organic media.[10–12] Naphthalimide incorporated in the molecular assemblies would act as a probe to characterize its self-assembling behaviour and therefore give some insight into the manner of molecular assembly. Prior to the fluorescence measurements, UV-Vis spectra were recorded in order to determine the excitation wavelength (λ_{exc}) and to correct the fluorescence emission intensity (see Fig. S1 in ESI†). The non-corrected fluorescence spectra of **2** in toluene at different concentrations from 0.01 wt% (solution) to 0.25 wt% (gel state) are given in Fig. 2a (λ_{exc} = 378 nm). One can notice a shift to shorter wavelength (blue-shift, hypsochromic effect) when the concentration increases. Fig. 3 shows the variation of the fluorescence maximum wavelength and the corrected (by the corresponding UV absorbance) fluorescence intensity of **2** in toluene at different concentrations. This has been compared to a model molecule (ref. **A**, Chart 1) which is an *N*-acylaminonaphthalimide. No variation can be observed for the model molecule whereas a 10 nm blue-shift of the maximum wavelength and a decrease of the corrected fluorescence intensity at a concentration of about 3.2 mM are detected for **2**. This would indicate some organization of naphthalimide above the CGC of **2**, contributing to the gelation phenomenon.

Fig. 2b shows the fluorescence spectra of **2** in toluene, recorded at different temperatures. The fluorescence emission maximum is shifted to longer wavelength when the temperature is above 40 °C. At the same time, an increase in the fluorescence intensity at around 40 °C (data not shown) suggests that the loose gel is transformed into an isotropic solution at this temperature. This observation is in good agreement with the work of Terech *et al.*,[13] who observed a 20 nm bathochromic shift of 2,3-di-*n*-decyloxy-6,7-dichloroanthracene when they recorded fluorescence spectra as a function of the temperature between −70 and 18 °C.

It has already been reported that fluorescence emission depends on the aggregation morphology such as H-type or J-type aggregation.[14] H-Aggregates correspond to molecules which are aligned parallel to each other with strong intermolecular interaction and induce non-radiative deactivation processes,[15] whereas J-aggregates are attributed to molecules that are arranged in a head-to-tail fashion and induce a relatively

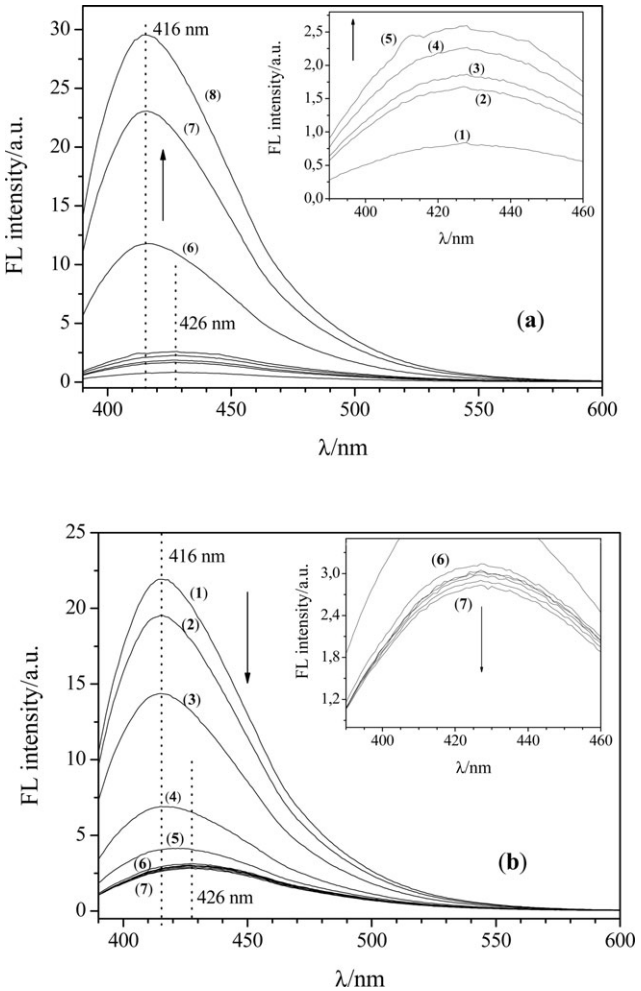

Fig. 2 Non-corrected fluorescence (FL) emission spectra of **2** in toluene at: (a) different concentrations, at 25 °C; ↑: increasing concentration ((1) −0.05, (2) −0.09, (3) −0.11, (4) −0.13, (5) −0.15, (6) −0.18, (7) −0.21 and (8) −0.25 wt%) and (b) different temperatures for the concentration of 0.21 wt%; ↓: increasing temperature ((1) −25, (2) −30, (3) −35, (4) −40, (5) −42, (6) −44, 46, 48, 50, 55 and (7) −60 °C) (λ_{exc} = 378 nm).

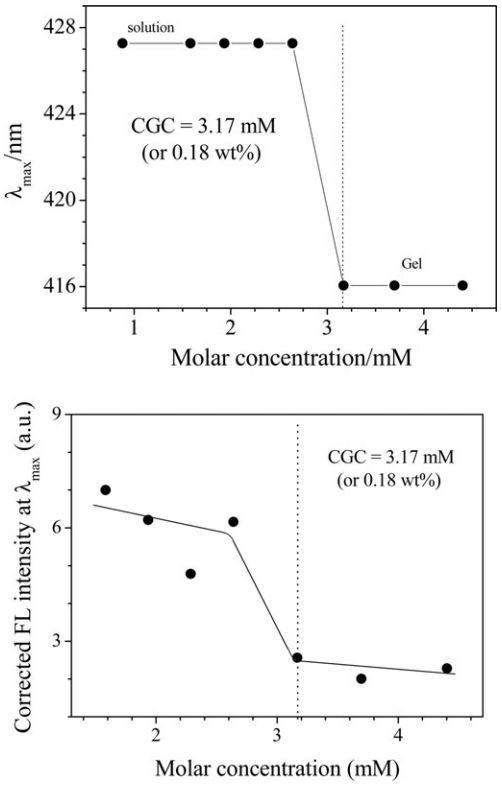

Fig. 3 Variation of (a) the fluorescence maximum wavelength and (b) the corrected fluorescence (FL) intensity of **2** in toluene as a function of the concentration.

high fluorescence efficiency.[16] Our results suggest that the molecules **2** are aligned parallel to each other and form H-aggregates in toluene.

Very surprisingly, in the case of **1** in toluene, the fluorescence maximum is shifted to shorter wavelength when the gel melts into an isotropic solution, as shown in Fig. 4a. In other words, when aggregates are formed from ''single'' molecules, by effect of the concentration or temperature, a red-shift, accompanied by an enhanced fluorescence signal, is observed. This would indicate a J-aggregate structure. This result is probably linked to the nature of the side chain R which, in the case of **2**, can participate in intermolecular interactions *via* π-stacking, leading to the formation of H-aggregates, which is not the case for **1**. This will be discussed in more detail in the molecular modelling part.

We also studied the influence of the solvent with respect to the manner of molecular assembly. A mixture of toluene and CCl_4 were chosen, due to their identical dielectric constant (an important point for the CD study, see next part) and apolar nature (no H-bonds possible). Fig. 4(b and c) show the fluorescence spectra for **1** and **2** in a toluene–CCl_4 mixture (v/v: 1/1) at different temperatures. When the gel is transformed into an isotropic solution, one can recognize that the fluorescence maximum wavelength remains almost unchanged for **2** but still shifts to shorter wavelength for **1**, as observed in pure toluene. We suppose that the presence of CCl_4 may stabilize a J-aggregate configuration. As a consequence, a mixture of H- and J-type aggregates should co-exist within the self-assembly of **2**, leading to an unchanged fluorescence maximum wavelength. In case of **1**, the CCl_4 reinforces the existence of J-aggregates.

Two-photon imaging is a non-linear approach well suited for deep-tissue and *in vivo* imaging of live animals but can be also used for imaging fluorescent macromolecules.[17] Among the experimental methods that have been developed to study macromolecular organization, second harmonic generation (SHG) is widely used due to its high sensitivity. Nevertheless and to the best of our knowledge, this technique has never been employed to study organogelators. Moreover, as processes involved in multiphoton fluorescence and SHG are intrinsic properties of the constituent molecules, non-linear microscopy allows submicron resolution images without the need for sectioning or staining with dye. Since SHG is a coherent elastic process which is dependent on the polarization of the incident light, SHG requires polarizable material with non-centrosymmetric symmetry; the greatest intensity SHG

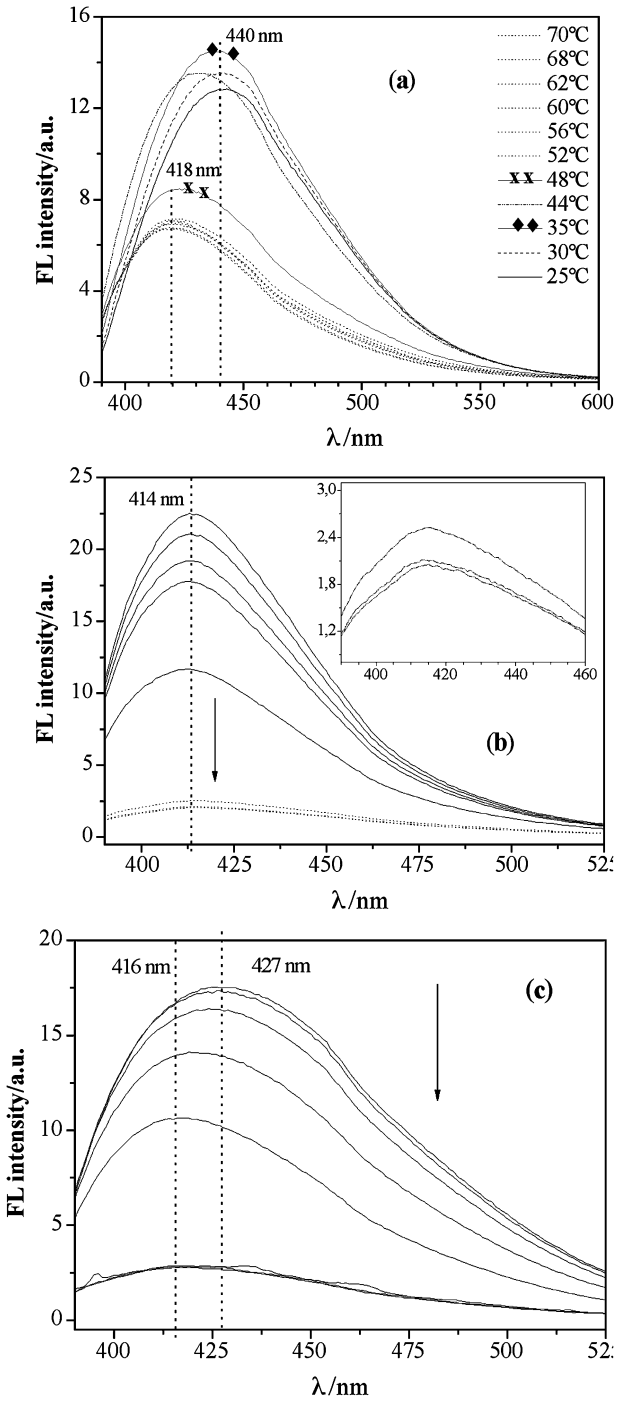

Fig. 4 Fluorescence emission spectra of: (a) **1** in toluene (0.8 wt%) at different temperatures; (b) **2** and (c) **1** in toluene + CCl_4 (v/v: 1/1) at different temperatures for the concentration of 0.25 wt%. ↓: increasing temperature (25, 35, 45, 50, 60, 70, 75 and 80 °C) (λ_{exc} = 378 nm).

signal is detected when the molecules are oriented parallel to the laser polarization.

Prior to the observation, we measured SHG signals from the model molecule (ref. **A**) in toluene and from an isotropic solution of gelator **2** in toluene (0.05 wt%). As expected, no SHG signals were detected which is consistent with a non-structured system. In Fig. 5a, fluorescence and SHG images of

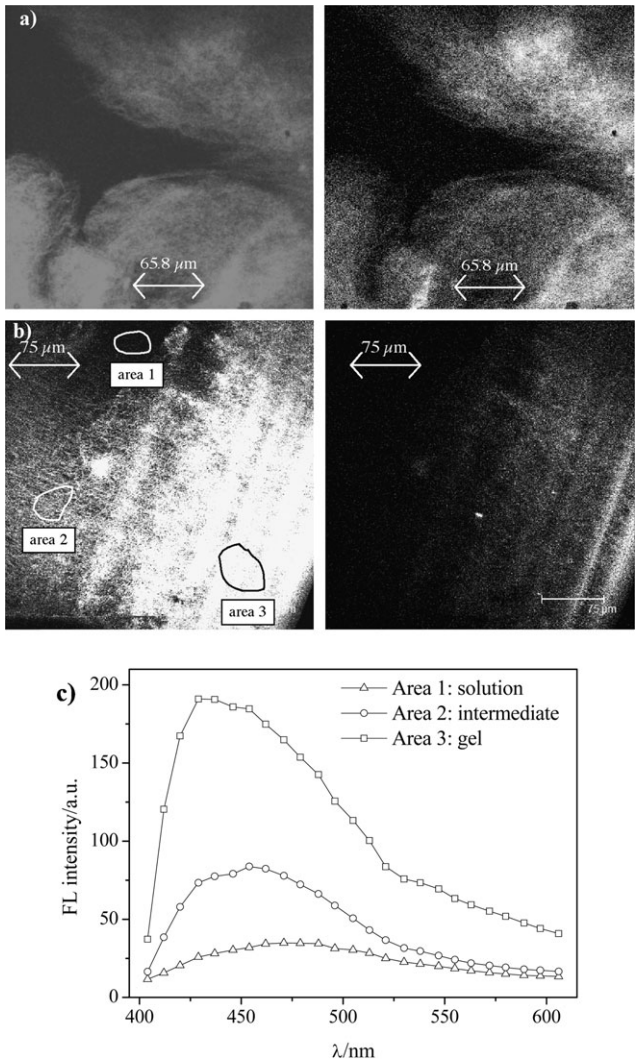

Fig. 5 Fluorescence (left) and SHG (right) images of **2** in toluene at different concentrations: (a) 0.25 wt%, (b) 0.15 wt%. (c) Fluorescence spectra of different areas of **2** (0.15 wt%) in toluene (λ_{exc} = 800 nm).

2 in toluene (0.25 wt%, gel state) are shown. We observe, with care, a fibrillar network.

This observation will be discussed in detail in the next part. On the other hand, we recognize a good correspondence between the fluorescence and SHG images, indicating a non-centrosymmetric structure. Moreover, SHG signals are distributed over the observed domain. This suggests that gelator molecules are locally well-ordered with one another in a parallel way. This result supports the data obtained from fluorescence and CD spectroscopies.

To analyze furthermore the molecular arrangement, we carried out experiments at an intermediate concentration (0.15 wt%). Logically, a small amount of solvent evaporation around the edges would result in a concentration gradient of **2** over the domain. At the edges, the local concentration should be equal to or a little higher than the critical gelation concentration, leading to local gel formation. Fig. 5b shows fluorescence and SHG images of such a sample. As expected, an intensity gradient of SHG signals is observed, following the concentration gradient. This confirms the eventual ordering of

the molecular arrangement into a fibrillar network when the gelator concentration is high enough. Furthermore, we recorded the fluorescence emission spectra of different regions, from the isotropic solution to the gel state for this sample. The λ_{max} of the gel region is blue-shifted compared to the solution region, as we observed by fluorescence spectroscopy (Fig. 5c).

3 CD spectroscopic results

CD is an efficient technique for the study of the chiral orientation of gelator molecules inside the gel. In general, there is a direct correlation between the regions of absorption and CD. In the case of non-coupled chromophores, the shapes of the two spectra are similar, although the vibrational fine structure can be different. If two or more strongly absorbing chromophores are oriented chirally with respect to each other, an exciton spectrum is observed and the λ_{max} in absorption corresponds, or nearly corresponds, to zero CD intensity.[18] The latter case is rather frequent during the formation of helical aggregates which are the common basis of gel formation by chiral gelators. During the self-assembly processes leading to gel formation, the CD spectrum undergoes dramatic modifications. Instructive examples of the appearance of exciton spectra during gelation have been reported by Shinkai *et al.*[19] Before gelation (in the solution state), the spectra in the region of azo chromophore absorption are flat; after gelation, an exciton pattern appears.

The CD spectra of **2** in toluene at different temperatures are given in Fig. 6a. It was confirmed that the contribution of linear dichroism (LD) spectra to the CD spectra is negligible. The UV absorption λ_{max} values appear at around 365 nm which corresponds to an $n \rightarrow \pi^*$ electron transition of the naphthalimide moiety.[20,21] In the CD spectra, the $\lambda_{\theta=0}$ values appear at 370 nm. One can therefore assign the CD spectra to the exciton coupling bands. At 25 °C (gel state), the CD spectrum of **2** in toluene exhibits a negative sign for the first Cotton effect ($[\theta]_{378} = -1.48\ 10^{-4}$ deg M^{-1} cm^{-1}), indicating that the dipole moments (in the naphthalimide chromophores) orientate in an anticlockwise direction in the aggregate (left-handed helical structure).[22–24] Moreover, the intensity of the CD signal decreases with an increase of the temperature suggesting a progressive destructuring of the superstructure. The CD peaks disappears at 45 °C as the loose gel is transformed into an isotropic solution. The disappearance of the CD signal in the solution leads us to conclude that the strong induced CD band originates from a chiral structure of the gel-aggregate, but not from a chiral conformation of **2** itself.[25]

The CD spectra of **1** in toluene at different temperatures show the same characteristics, with a negative sign for the first Cotton effect ($[\theta]_{379} = -0.37 \times 10^{-4}$ deg M^{-1} cm^{-1}). However, the CD spectra at RT (gel state) of gelators **1** and **2** in a toluene + CCl_4 (v/v: 1/1) solvent mixture change completely with a positive sign for the first Cotton effect (for **1**: $[\theta]_{383} = 0.98 \times 10^{-4}$ deg M^{-1} cm^{-1}, for **2**: $[\theta]_{381} = 1.33 \times 10^{-4}$ deg M^{-1} cm^{-1}), as shown in Fig. 6b. According to the literature,[5,26] solvent sometimes plays an important role in the shape of the CD spectra (changing the solvent leads to a shift of the wavelength of the maximum or a modification of the dichroism signal intensity). In such a case, polar solvents, like methanol, may form hydrogen bonds with studied chromophores. Besides, Moscowitz *et al.*[27] reported the effect of the dielectric constant of the solvent on the Cotton effect. In our studies, the dielectric constant of both toluene and CCl_4 is relatively low (at 76 °F (24.4 °C), $\varepsilon = 2.4$ for toluene and 2.2 for CCl_4) and they could not form H-bonds with C=O

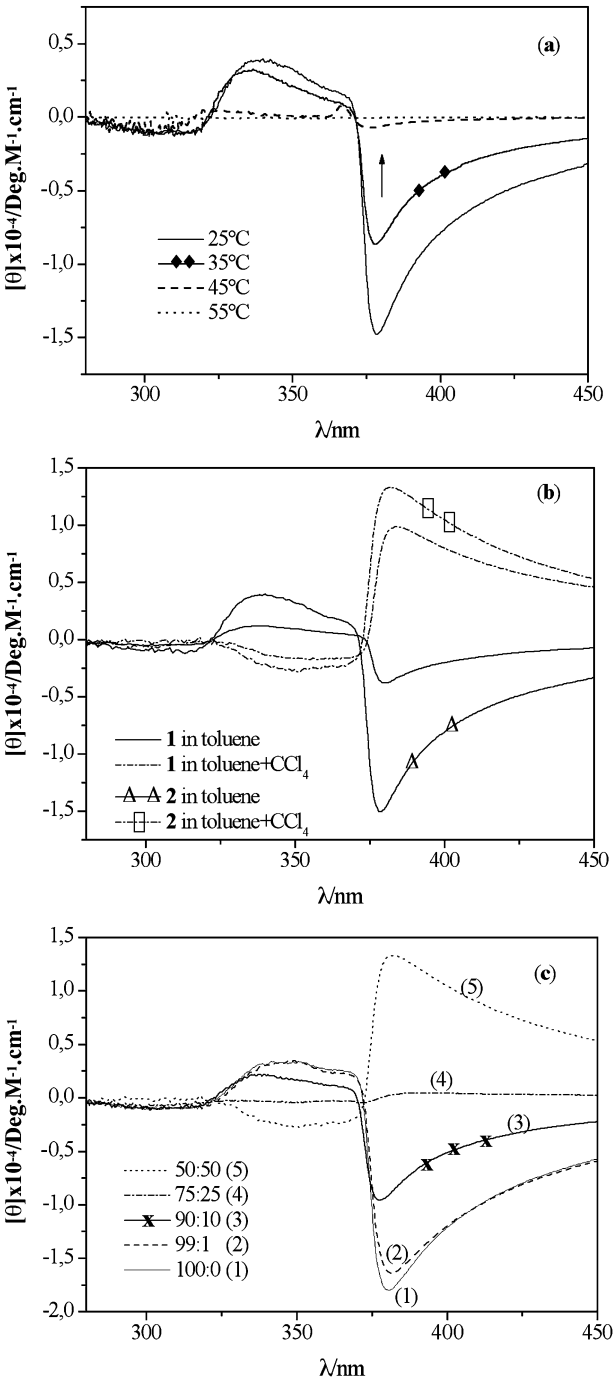

Fig. 6 (a) Temperature-dependent CD spectra of gelator **2** (0.20 wt%) in toluene. (b) CD spectra of gelators **1** and **2** in different solvents (toluene or toluene–CCl_4, v/v: 1/1, mixture) at 25 °C. (c) CD spectra of **1** in toluene + CCl_4 (1.7 mg mL^{-1}) of different proportions ($V_{toluene} : V_{CCl_4}$), at 25 °C.

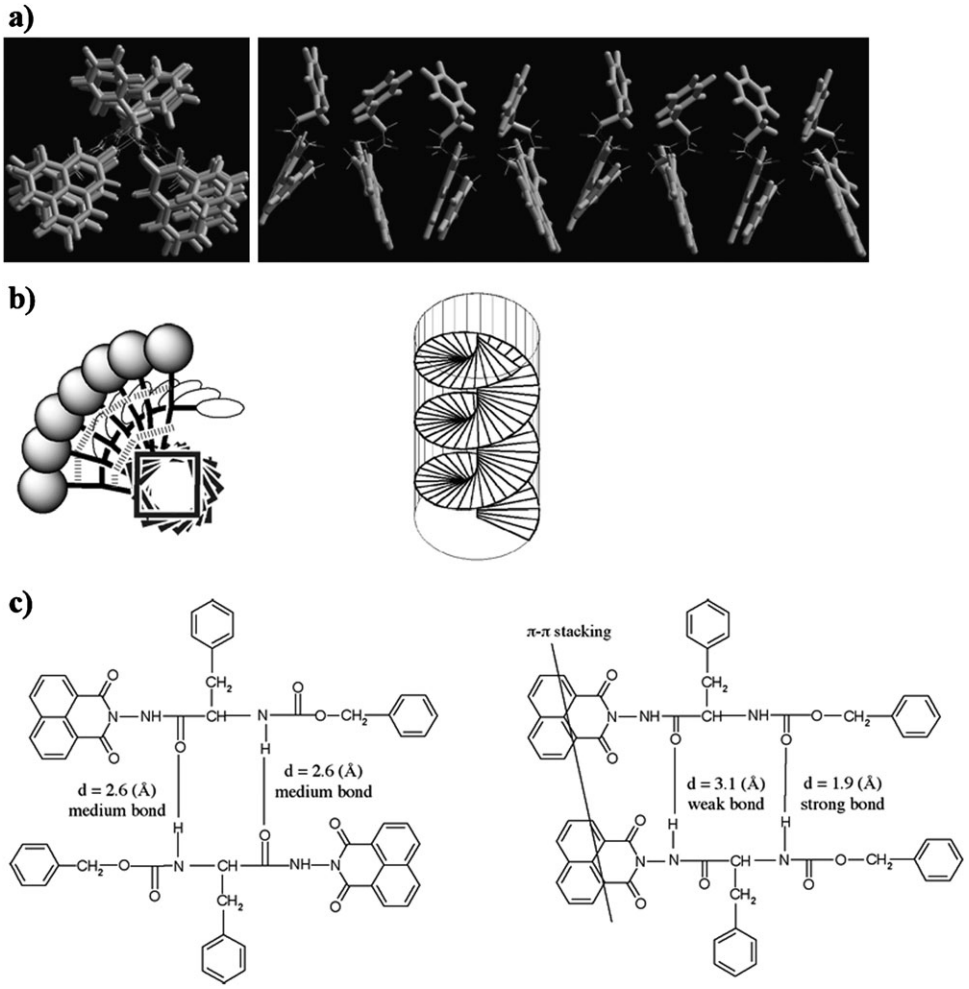

Fig. 7 (a) The stacking model of the octamer of **2** as a top-view (left) and edge-on-view (right); (b) helical arrangement with π-stacking interactions of naphthalimide moieties (square); (c) scheme of H-bonds for head-to-tail (left) and tail-to-tail (right) configurations in the dimer.

groups, so the main contribution probably comes from the fact that one is aromatic and the other is not. The presence of CCl_4 stabilizes the molecular arrangement which leads to an inversion of the Cotton effect. In all studied cases, these strong CD peaks disappear as the loose gel is transformed into an isotropic solution. Since this CD signal is, as above, derived from exciton coupling among the organized chromophore,[28] it is thought that the molecules **1** and **2** in toluene–CCl_4 solvent are cooperatively stacked helically with the naphthalimide moieties regularly orienting one another in a clockwise direction in the aggregate (right-handed helical structure). This interesting result shows the important role of solvent in relation to the molecular arrangement of gelators **1** and **2**, as confirmed by NMR studies.[29] To the best of our knowledge, no case in the literature of the organogel domain shows such a solvent effect: an achiral solvent can help to control the chirality of organogels. In the field of polymer gels, few articles showed a possible transition between left- and right-handed helices generated by the changes in solvation or temperature.[30] Some authors proposed that the presence of another solvent kind might influence the entropy of these two conformations (left- and right-handed helices). But the exact mechanism is still obscure.

In order to better understand this phenomenon, we performed CD measurements of **2** (1.7 mg mL^{-1}) in toluene + CCl_4 at different volume proportions, as shown in Fig. 6c. It is clear that CD signal intensity decreases with increasing CCl_4 volume and is reversed, the Cotton effect changing from a negative sign to a positive one. By controlling the CCl_4 volume, we could modify the chirality of self-assembled aggregates. This result is very interesting for diverse applications.[22,23]

4 Energetics and geometry

At the PM3MM level, the head-to-tail dimer is slightly (4.3 kcal mol^{-1} for **2**, and 2.7 kcal mol^{-1} for **1**) less stable than the tail-to-tail one. The head-to-tail octamer is also less stable than the tail-to-tail one, and by a significant 22.8 kcal mol^{-1} for **2**, but only 1.2 kcal mol^{-1} for **1**. We can thus conclude that, in a vacuum, the superstructure clearly seems to prefer a tail-to-tail position for **2**, and that the situation is more ambiguous for **1**. From the octamer structure, we can observe (Fig. 7a) that the head-to-tail structure stacks vertically in a symmetrical fashion, whereas the tail-to-tail structure stacks with a slight shift for each monomer, resulting in a

helicoid superstructure (Fig. 7b). The latter is thus a chiral structure, and this is in agreement with the circular dichroism experimental results. We can also notice in the tail-to-tail superstructure that not all the aromatic rings seem to stack. In fact, the naphthalimide and aromatic part of the phenyl side chain of **2** are stacked together, but in contrast, the phenyl moieties of the –O–CO–CH_2–C_6H_5 protecting group seem to adopt a rather disordered arrangement. This could be a hint that **2** prefers the tail-to-tail structure because a favourable π-stacking interaction includes the naphthalimide AND phenyl moieties, whereas **1** (for which the tail-to-tail structure is not so energetically favoured) can only π-stack the naphthalimide moieties.

The intermolecular forces that are responsible for the stacked superstructures can be analyzed in the dimer study. Between aromatic rings, π-stacking is certainly playing an important role for favourable interactions between molecules. This is the case where the aromatic rings are generally coplanar, *i.e.* for the naphthalimide moieties (and phenyl moieties for **2** but not **1**), but not the benzyl ones.

Apart from π-stacking, intermolecular hydrogen bonding also plays an important role. In the head-to-tail structure, two superimposed molecules are linked together with the help of two strong (Fig. 7c) N–H···O hydrogen bonds. This feature leads to a conformation analogous to a peptide β-sheet antiparallel hydrogen bond network, a notoriously stable one. In the tail-to-tail structure, the intermolecular hydrogen bonding network is obviously less efficient. One hydrogen bond possesses geometrical characteristics of a stable, strong one, but the other one is certainly very loose. This network looks like the parallel β-sheet peptide hydrogen bond network. Thus, the tail-to-tail structure is the most stable, but possesses a less efficient intermolecular hydrogen bonding network. It is thus pivotal to explain the stability of this structure by better π-stacking, which compensates for the weaker intermolecular hydrogen bonding network.

5 Observation of fibrillar network in gel state and in dried samples

Fig. 8 shows an *in situ* fluorescence image of gel **2** in toluene (0.25 wt%). We observe a molecular arrangement of **2** through a fibrillar network.

The TEM images of dried samples in Fig. 9 show many juxtaposed fibrous aggregates whose diameters are *ca.* 25–200 nm. As yet, helical aggregates, as expected from CD spectroscopic results, are not observed with TEM. Considering the fact that the width of the fibrous aggregates in the TEM is quite large compared to the molecular length of **2**, the huge fibrous aggregates in the TEM seem to be built up *via* a process of accumulation and rearrangement of "helical" smallest units.[25] Besides, the computational modelling was performed in vacuum conditions and this is probably one reason for the larger difference between the diameters of the fibers and the molecular length. There should be a solvent-dependent secondary aggregation mechanism (lateral growth or bundling mechanisms). On the other hand, these fibrous aggregates fit well with the result obtained from the fluorescence image. This confirms that the drying process, by using supercritical CO_2, does not change the morphology of the molecular organization in the gel state.

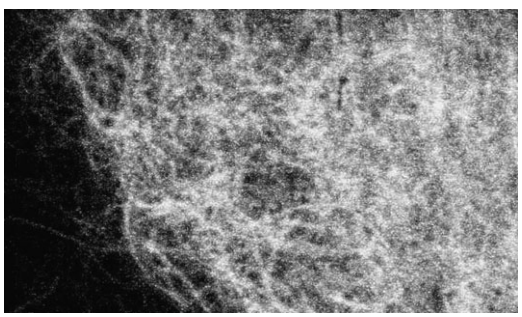

Fig. 8 Fluorescence image of gelator **2** in toluene (0.25 wt%, gel state).

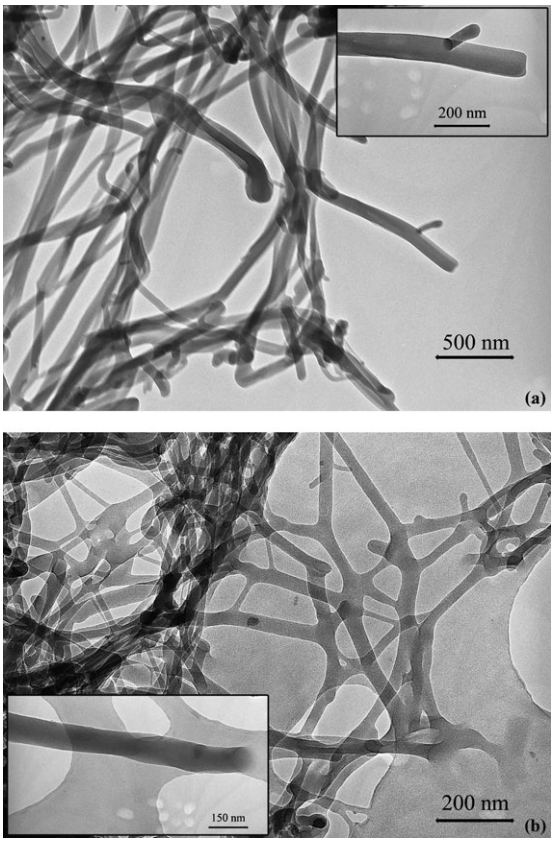

Fig. 9 TEM image of the aerogels (organogels, in toluene, dried by using supercritical CO_2): (a) gelator **1** and (b) gelator **2**.

Conclusions

The spectroscopic results obtained suggested that the molecules **1** and **2** can both stack into a fibrous structure. Regarding the nature of these molecules, the stacking phenomena can be explained by an H-bond network but also by π–π interactions. The nature of the side chain of **1** and **2** strongly influenced the organization of the aggregates, which is in an H-type for **2** in toluene and J-type for **1** in toluene. More surprisingly, we demonstrated by performing CD analyses that the nature of the solvent reversed the chirality of the aggregates. Indeed, we were able to observe, with the help of

SHG and fluorescence imaging techniques, a fibrillar network of a low molecular weight organogel without preliminary drying.

Experimental section

Synthesis

Compounds **1** and **2** (Chart 1) were prepared in three steps from (L)-amino acid methyl esters according to a general procedure described previously.[9]

Compound **1**. ^{1}H NMR (300 MHz, $CDCl_3$): δ 9.53 (s, 1H), 8.51–7.96 (m, 4H), 7.68–7.07 (m, 7H), 5.83 (d, 1H), 5.07 (dd, 1H), 5.02 (dd, 1H), 4.80–7.30 (m, 1H), 2.04–1.66 (m, 3H), 1.00 (s, 6H). ^{13}C NMR ($CDCl_3$): δ 172.3, 162.7, 162.2, 157.4, 136.8, 135.1, 132.2, 132.0, 128.9, 128.4, 128.2, 127.3, 122.7, 67.6, 52.6, 41.6, 25.2, 23.5, 22.6. Anal. Calcd for $C_{26}H_{25}N_3O_5$: C, 67.69; H, 4.48; N, 9.14. Found: C, 68.05; H, 4.62; N, 9.46%.

Compound **2**. ^{1}H NMR (300 MHz, $CDCl_3$): δ 8.85 (s, 1H), 8.65–8.45 (m, 2H), 8.20 (d, 2H), 7.80–7.60 (m, 2H), 7.45–7.10 (m, 10H), 5.63 (m, 1H), 5.15–5.00 (m, 2H), 5.00–4.75 (m, 1H), 3.38 (dd, 1H), 3.18 (dd, 1H). ^{13}C NMR ($CDCl_3$): δ 170.6, 161.7, 155.9, 136.9, 136.5, 134.7, 131.7, 131.6, 129.7, 129.5, 128.4, 128.3, 127.9, 127.7, 127.0, 126.6, 122.1, 66.2, 54.6, 38.6. Anal. Calcd for $C_{29}H_{23}N_3O_5$: C, 70.58; H, 4.70; N, 8.51. Found: C, 70.28; H, 4.72; N, 8.46.

Preparation of the gels

The gels were prepared by heating the solvent and the organogelator (0.18–3 wt%) in a flask fitted with a reflux condenser until the complete dissolution of the solid. The solution was transferred into a closed vial and cooled to 4 °C. Most of the time, the formation of the gel occurred within several minutes.

Melting temperatures

This parameter, used to establish the "temperature–concentration" phase diagram, was obtained with the "falling ball" method.[31] The technique used a steel ball (4 mm diameter, 0.2607 g) immersed in the gel contained in a test tube (11 mm diameter). The ball was positioned at the center of the tube. At the melting transition, the ball dropped down to the bottom of the tube. For each concentration, the experiments were repeated at least three times.

Instrumentation

Absorption spectra were recorded on a Perkin-Elmer (Lambda 2, Courtaboeuf, France) UV-visible spectrophotometer. Fluorescence spectra were recorded on a SPEX Fluorolog-3 spectrofluorimeter (Jobin Yvon, Longjumeau, France) equipped with a thermostated cell compartment, using a 450 W xenon lamp. The gel samples were directly prepared in quartz cells having a 2 mm optic path length. CD spectral measurements were performed using a Jobin Yvon CD6 spectrometer.

Concerning the fluorescence microscopy with multiphoton excitation, short infrared pulses (λ = 800 nm) were generated from a femtosecond oscillator (Mira 900F from 600 to 1100 nm, Coherent), pumped with a solid laser (Verdi 8 W, Coherent). An EOM (electro optical modulator LM 0202 P 5W-n°21181, EO-Crystal KD*P 3 × 3 mm^2, 5 W, 660–1050 nm, transmission 90.1%, ratio 1/254)) enabled control of the power of excitation (2.5 nJ per pulse at 76 MHz). The laser beam was focalized on the samples through an objective showing ×20 magnification (dry, numerical aperture NA = 0.7). A confocal laser scanning microscope (TCS SP2-AOBS, Leica Microsystems combined with multiphoton excitation), pinhole fully opened (Airy 49.46), enabled to obtain images in 512 × 512 matrices at 400 Hz (1 pixel = 146 nm). 16 frames with a line average of 2 were accumulated to improve quality of images.

The second harmonic signal was measured through an ×40 objective (NA = 0.8, dry), at the half of the wavelength of the excitation ($\lambda/2$ = 400 nm) in the forward direction (transmitted light channel). A band-pass filter enabled selection of the detection spectral range (400 ± 25 nm), and a low-pass filter rejection of the infrared excitation beam (800 nm).

For transmission electron microscopy (TEM), the dry organogel samples (aerogels), obtained *via* a drying process using a CO_2 supercritical fluid,[9] were dispersed into water and deposed on a Cu grid covered with a holey carbon film. After drying, the grid was introduced in a CM20 Philips electron microscope operating at 200 kV.

Computational details

Calculations were performed at the CINES calculation center with the Gaussian 03 version C.02 package[32] with default conditions. The geometry optimization of two dimer conformations (hereafter referred to as head-to-tail and tail-to-tail structures) of **1** and **2** was performed using the PM3MM semi-empirical level[33] and the B3LYP/6-31G (d,p)[34] density functional level of theory. Minima were checked successfully for consistent positive vibration frequencies. From these dimers, two superstructures of eight stacked molecules were built and then submitted to a geometry optimization at the semi-empirical PM3MM level. The presence of hydrazino N–N bonds in the studied molecules prevented us from using a molecular mechanics geometry optimization. As a matter of fact, no force-field to date correctly represents the internal rotation around the C–N–N–C bond, predicting a minimum in a flat conformation, whereas any quantum mechanical method correctly predicts a minimum torsional angle around 90°.

It should be noted that our computational study was performed *in a vacuum*, *i.e.* without any solvent surrounding our stacked molecules. This study is thus NOT intended to recreate the conditions in which organogel molecules could organize. Rather, it was performed to determine structural information on a molecular stacked superstructure, in agreement with experimental evidence like proton NMR (for intermolecular hydrogen bonding network), or circular dichroism (for superstructure chirality).

Acknowledgements

The authors gratefully thank J.-P. Desvergne for his helpful discussion about UV and fluorescence spectroscopies. Circular dichroism experiments were conducted at the "Service

Commun de Biophysicochimie des Interactions Moléculaires" of Université Henri Poincaré, Nancy-Université.

References

1. (*a*) P. Terech and R. G. Weiss, *Chem. Rev*., 1997, **97**, 3133; (*b*) *Molecular Gels*, ed. R. G. Weiss and P Terech, Springer, Dordrecht, Netherlands, 2006; (*c*) selection of recent papers: M. Moniruzzaman and P. R. Sundararajan, *Langmuir*, 2005, **21**, 3802; (*d*) X. Huang, P. Terech, S. R. Raghavan and R. G. Weiss, *J. Am. Chem. Soc*., 2005, **127**, 4336; (*e*) R. Schmidt, F. B. Adam, M. Michel, M. Schmutz, G. Decher and P. J. Mésini, *Tetrahedron Lett*., 2003, **44**, 3171; (*f*) M. Suzuki, T. Nigawara, M. Yumoto, M. Kimura, H. Shirai and K. Hanabusa, *Tetrahedron Lett*., 2003, **44**, 6841.
2. (*a*) G. Haering and P. L. Luisi, *J. Phys. Chem*., 1986, **90**, 5892; (*b*) R. J. Phillips, W. M. Deen and J. F. Brady, *J. Colloid Interface Sci*., 1990, **139**, 363; (*c*) J. Eastoe, M. Sanchez-Dominguez, P. Wyatt and R. K. Heenan, *Chem. Commun*., 2004, 2608; (*d*) R. J. H. Hafkamp, B. P. A. Kokke, I. M. Danke, H. P. M. Guerts, A. E. Rowan, M. C. Feiters and R. J. M. Nolte, *Chem. Commun*., 1997, 545.
3. (*a*) P. Terech, D. Pasquier, V. Bordas and C. Rossat, *Langmuir*, 2000, **16**, 4485; (*b*) M. George and R. G. Weiss, *Chem. Mater*., 2003, **15**, 2879.
4. D. Hamada, I. Yanagihara and K. Tsumoto, *Trends Biotechnol*., 2004, **22**, 93.
5. Y. Jeong, K. Hanabusa, H. Masunaga, I. Akiba, K. Miyoshi, S. Sakurai and K. Sakurai, *Langmuir*, 2005, **21**, 586.
6. (*a*) J. Becerril, K. Hanabusa, K. Okui, K. Karaki, T. Koyama and H. Shirai, *J. Chem. Soc., Chem. Commun*., 1992, 1371; (*b*) A. Carré, P. Le Grel and M. Baudy-Floc'h, *Tetrahedron Lett*., 2001, **42**, 1887; (*c*) J. Makarevic, M. Jokic, L. Frkanec, D. Katalenic and M. Zinic, *Chem. Commun*., 2002, 2238; (*d*) S. Okabe, K. Ando, K. Hanabusa and M. Shibayama, *J. Polym. Sci., Part B: Polym. Phys*., 2004, **42**, 1841; (*e*) H. Ihara, T. Sakurai, T. Yamada, T. Hashimoto, M. Takafuji, T. Sagawa and H. Hachisako, *Langmuir*, 2002, **18**, 7120; (*f*) M. Suzuki, T. Sato, A. Kurose, H. Shirai and K. Hanabusa, *Tetrahedron Lett*., 2005, **46**, 2741.
7. K. Hanabusa, K. Okui, K. Karaki, M. Kimura and H. Shirai, *J. Colloid Interface Sci*., 1997, **195**, 86.
8. (*a*) J. van Esch, F. Schoonbeek, M. de Loos, H. Kooijman, A. L. Spek, R. M. Kellogg and B. L. Feringa, *Chem.–Eur. J*., 1999, **5**, 937; (*b*) J. Brinksma, B. L. Feringa, R. M. Kellogg, R. Vreeker and J. van Esch, *Langmuir*, 2000, **16**, 9249; (*c*) A. D. Hamilton and G. Wang, *Chem.–Eur. J*., 2002, **8**, 1954; (*d*) P. Babu, N. M. Sangeetha, P. Vijaykumar, U. Maitra, K. Rissanen and A. R. Raju, *Chem.–Eur. J*., 2003, **9**, 1922.
9. N. Brosse, D. Barth and B. Jamart-Gregoire, *Tetrahedron Lett*., 2004, **45**, 9521.
10. C. Nouvel, C. Frochot, V. Sadtler, P. Dubois, E. Dellacherie and J. L. Six, *Macromolecules*, 2004, **37**, 4981.
11. H. Bouas-Laurent and J.-P. Desvergne, in *Molecular Gels*, ed. R. G. Weiss and P Terech, Springer, Dordrecht, Netherlands, 2006, ch. 12, pp. 363–429.
12. T. Sagawa, S. Fukugawa, T. Yamada and H. Ihara, *Langmuir*, 2002, **18**, 7223.
13. P. Terech, D. Meerschaut, J. P. Desvergnes, M. Colomes and H. Bouas-Laurent, *J. Colloid Interface Sci*., 2003, **261**, 441.
14. (*a*) B. K. An, S. K. Kwon, S. D. Jung and S. Y. Park, *J. Am. Chem. Soc*., 2002, **124**, 14410; (*b*) B. K. An, D. S. Lee, J. S. Lee, Y. S. Park, H. S. Song and S. Y. Park, *J. Am. Chem. Soc*., 2004, **126**, 10232; (*c*) E. G. McRae and M. J. Kasha, *Chem. Phys*., 1958, **28**, 721; (*d*) N. C. Maiti, S. Mazumdar and N. Periasamy, *J. Chem. Phys. B*, 1998, **102**, 1528; (*e*) U. Rosch, S. Yao, R. Wortmann and F. Wurthner, *Angew. Chem., Int. Ed*., 2006, **45**, 7026.
15. J. B. Birks, *Photophysics of Aromatic Molecules*, Wiley, London, 1970.
16. W. I. Gruszecki, *J. Biol. Phys*., 1991, **18**, 99.
17. M. Oheim, D. J. Michael, M. Geisbauer, D. Madsen and R. H. Chow, *Adv. Drug Delivery Rev*., 2006, **58**, 788.
18. G. Gottarelli, G. P. Spada and E. Castiglioni, in *Molecular Gels*, ed. R. G. Weiss and P Terech, Springer, Dordrecht, Netherlands, 2006, ch. 13, pp. 431–446.
19. K. Murata, M. Aoki, T. Suzuki, T. Hatada, H. Kawabata, T. Komori, F. Ohseto, K. Ueda and S. Shinkai, *J. Am. Chem. Soc*., 1994, **116**, 6664.
20. E. Martin, J. L. G. Coronado, J. J. Camacho and A. Pardo, *J. Photochem. Photobiol. A: Chem*., 2005, **175**, 1.
21. A. Demeter, T. Berces, L. Biczok, V. Wintgens, P. Valat and J. Kossanyi, *J. Phys. Chem*., 1996, **100**, 2001.
22. J. H. Jung, H. Kobayashi, M. Masuda, T. Shimizu and S. Shinkai, *J. Am. Chem. Soc*., 2001, **123**, 8785.
23. J. H. Jung, Y. Ono and S. Shinkai, *Chemistry*, 2000, **6**, 4552.
24. K. Sugiyasu, N. Fujita and S. Shinkai, *Angew. Chem., Int. Ed*., 2004, **43**, 1229.
25. K. Hanabusa, H. Kobayashi, M. Suzuki, M. Kimura and H. Shirai, *Colloid Polym. Sci*., 1998, **276**, 252.
26. P. Crabbé, *Applications de la Dispersion Roratoire Optique et du Dichroïsme Circulaire Optique en Chimie Organique*, Gauthier-Villars, Paris, 1968, ch. 6, pp. 317–358.
27. A. Moscowitz, K. M. Wellman and C. Djerassi, *Proc. Natl. Acad. Sci. USA*, 1963, **50**, 799.
28. A. Rodger and B. Norden, *Circular Dichroism and Linear Dichroism*, Oxford University Press, Oxford, 1996.
29. Q. N. Pham, N. Brosse, B. Jamart-Gregoire, H. Yemloul and D. Canet, in preparation. The NMR data show that, for toluene + CCl_4 solvent, two protons in the *ortho* position of the naphthalimide moiety of gelators become inequivalent in gel state. This would mean that this solvent mixture favors the π-stacking interactions between naphthalimide moieties in the gel state.
30. (*a*) K. Morino, K. Maeda and E. Yashima, *Macromolecules*, 2003, **36**, 1480 and therein; (*b*) H. Nakako, R. Nomura and T. Masuda, *Macromolecules*, 2001, **34**, 1496.
31. A. Takahashi, M. Sakai and T. Kato, *Polym. J*., 1980, **12**, 335.
32. M. J. Frisch, G. W. Trucks, H. B. Schlegel, G. E. Scuseria, M. A. Robb, J. R. Cheeseman, J. A. Montgomery, Jr., T. Vreven, K. N. Kudin, J. C. Burant, J. M. Millam, S. S. Iyengar, J. Tomasi, V. Barone, B. Mennucci, M. Cossi, G. Scalmani, N. Rega, G. A. Petersson, H. Nakatsuji, M. Hada, M. Ehara, K. Toyota, R. Fukuda, J. Hasegawa, M. Ishida, T. Nakajima, Y. Honda, O. Kitao, H. Nakai, M. Klene, X. Li, J. E. Knox, H. P. Hratchian, J. B. Cross, V. Bakken, C. Adamo, J. Jaramillo, R. Gomperts, R. E. Stratmann, O. Yazyev, A. J. Austin, R. Cammi, C. Pomelli, J. Ochterski, P. Y. Ayala, K. Morokuma, G. A. Voth, P. Salvador, J. J. Dannenberg, V. G. Zakrzewski, S. Dapprich, A. D. Daniels, M. C. Strain, O. Farkas, D. K. Malick, A. D. Rabuck, K. Raghavachari, J. B. Foresman, J. V. Ortiz, Q. Cui, A. G. Baboul, S. Clifford, J. Cioslowski, B. B. Stefanov, G. Liu, A. Liashenko, P. Piskorz, I. Komaromi, R. L. Martin, D. J. Fox, T. Keith, M. A. Al-Laham, C. Y. Peng, A. Nanayakkara, M. Challacombe, P. M. W. Gill, B. G. Johnson, W. Chen, M. W. Wong, C. Gonzalez and J. A. Pople, *GAUSSIAN 03 (Revision C.02)*, Gaussian, Inc., Wallingford, CT, 2004.
33. (*a*) J. J. P. Stewart, *J. Comput. Chem*., 1989, **10**, 209; (*b*) J. J. P. Stewart, *J. Comput. Chem*., 1989, **10**, 221.
34. (*a*) S. H. Vosko, L. Wilk and M. Nusair, *Can. J. Phys*., 1980, **58**, 1200; (*b*) A. D. Becke, *J. Chem. Phys*., 1993, **98**, 5648; (*c*) B. Miehlich, A. Savin, H. Stoll and H. Preuss, *Chem. Phys. Lett*., 1989, **157**, 200; (*d*) C. Lee, W. Yang and R. G. Parr, *Phys. Rev. B*, 1988, **37**, 785.